www.ptcer.pl/mccm

MATERIAŁY CERAMICZNE /CERAMIC MATERIALS/, 62, 4, (2010), 516-520

Microstructure, Thermal Behaviour and Luminescent Properties of Electrospun Eu-doped TiO_2 Nanofibres

Ilaria Cacciotti[1]*, Francesca Romana Lamastra[2], Alessandra Bianco[1], Adolfo Speghini[3] Fabio Piccinelli[4], Maria Elena Fragalà[5], Graziella Malandrino[5], Gualtiero Gusmano[1]

[1] University of Rome "Tor Vergata", Department of Chemical Science and Technology INSTM RU Tor Vergata, Via della Ricerca Scientifica, 00133 Rome, Italy
[2] Italian Interuniversitary Consortium on Materials Science and Technology (INSTM) Research Unit Roma Tor Vergata, Via della Ricerca Scientifica, 00133 Rome, Italy
[3] University of Verona, Solid State Chemistry Laboratory, DB, INSTM RU Verona Strada Le Grazie 15, 37134 Verona; Italy
[4] University of Verona, DiSTeMeV, INSTM RU Verona, Via della Pieve 70, 37029 S. Floriano (VR), Italy
[5] University of Catania, Department of Chemical Science, INSTM UR Catania Viale Andrea Doria 6, 95100 Catania, Italy
*e-mail: ilaria.cacciotti@uniroma2.it

Abstract

Pure and europium-doped titania nanofibers were successfully fabricated by the electrospinning technique, using a single multielement titanium/europium source. Eu content was 5 mol.%. Microstructure was studied by means of scanning electron microscopy (SEM), thermal behaviour followed by thermogravimetric and differential thermal analysis (TG-DTA). Phase analysis was performed by means of X-ray diffraction (XRD) and high temperature X-ray diffraction analysis (HT-XRD) up to 1100°C. Luminescence measurements were performed using a laser excitation source at 395 nm. All electrospun materials consisted of randomly oriented nanofibers of a fairly uniform diameter. The average fiber size was 80 ± 20 nm and 40 ± 10 nm for Eu-doped and undoped TiO_2 calcinated at 500°C, respectively. The presence of europium shifted toward higher values either the crystallization temperature of anatase and the anatase to rutile phase transition, the latter being accompanied by the formation of the $EuTi_2O_7$ phase. The doped samples show a strong luminescence of Eu^{3+} ions. The emission spectra are dominated by the $^5D_0 \rightarrow {}^7F_2$ emission, suggesting a notable distorsion around the Eu^{3+} ions. The broadening of the bands points to the presence of a relevant inhomogeneous disorder around the Eu^{3+} sites.

Keywords: Titania, Nanofibres, Electrospinning, Microstructure

MIKROSTRUKTURA, WŁAŚCIWOŚCI CIEPLNE I LUMINESCENCJA NANOWŁÓKIEN TiO_2 DOMIESZKOWANYCH EUROPEM, OTRZYMANYCH METODĄ PRZĘDZENIA ELEKTROSTATYCZNEGO

Nanowłókna tlenku tytanu(IV), domieszkowane europem i bez domieszkowania, wytworzono z powodzeniem metodą przędzenia elektrostatycznego, wykorzystując pojedyncze, wielopierwiastkowe źródło tytan/europ. Zawartość europu wynosiła 5 % mol. Mikrostrukturę badano za pomocą skaningowej mikroskopii elektronowej (SEM), zachowanie podczas ogrzewania śledzono za pomocą analizy termograwimetrycznej i termicznej analizy różnicowej (TG-DTA). Analizę fazową przeprowadzono za pomocą dyfrakcji promieniowania X (XRD) i wysokotemperaturowej analizy dyfrakcyjnej promieniowania X (HT-XRD), aż do 1100°C. Pomiary luminescencyjne przeprowadzono wykorzystując laserowe źródło wzbudzenia przy 395 nm. Wszystkie elektrostatycznie przędzone materiały składały się z przypadkowo zorientowanych nanowłókien o raczej wyrównanej średnicy. W przypadku włókien TiO_2 kalcynowanych w 500°C średni rozmiar wynosił 80 ± 20 nm i 40 ± 10 nm, odpowiednio dla włókien domieszkowanych Eu i bez domieszkowania. Obecność europu przesunęła w stronę wyższych wartości zarówno temperaturę krystalizacji anatazu, jaki i temperaturę przemiany anatazu w rutyl, której to towarzyszyło tworzenie się fazy $EuTi_2O_7$. Próbki domieszkowane pokazały mocną luminescencję jonów Eu^{3+}. Widma emisyjne są zdominowane przez emisję $^5D_0 \rightarrow {}^7F_2$, co sugeruje znaczące odkształcenie wokół jonów Eu^{3+}. Poszerzenie pasm wskazuje na obecność odpowiedniego, niejednorodnego nieuporządkowania wokół miejsc przebywania Eu^{3+}.

Słowa kluczowe: tlenek tytanu(IV), nanowłókna, przędzenie elektrostatyczne, mikrostruktura

1. Introduction

Titanium dioxide (TiO_2) is widely employed in catalysis, sensors [1], photo-electrochemical cells, optical filters [2], solar cells and optoelectronic devices [3]. Moreover, due to its outstanding optical and thermal properties and high stability, TiO_2 is a good candidate to be used as a host material for rare-earth (RE) elements to prepare photoluminescent materials with promising applications in photoelectric devices and optical communication fields, *i.e.*, photoelectric devices, solid state laser materials, flat panel displays, high energy radiation detectors, optical data storage and even medical diagnostics [1-8]. Among them europium-doped oxides have excellent luminescent properties [9-10], making them

suitable to be used as light-emitting materials, both in the visible and in the near infrared range for many technological applications [11-14].

RE-doped titania nanopowders and thin films have been widely investigated and synthesised adopting hydrothermal procedures [3], solvothermal techniques [15], sol-gel methodologies [11], and low pressure hot target magnetron sputtering [2]. Although growing attention is devoted to TiO_2 nanofibers prepared by electrospinning technique [16-19], RE-doped TiO_2 nanofibers synthesised by electrospinning have been rarely investigated [6, 20-21, 22-24].

Electrospinning consists in an extremely flexible process, already scaled up for manufactures, able to fabricate continuous nanofibers from a huge range of materials [25].

In this work undoped and Eu-doped titania nanofibers were produced by means of the electrospinning technique, starting from polyvinylpyrrolidone, titanium tetraisopropoxide ($Ti(O\text{-}i\text{-}Pr)_4$ and $Eu(hfa)_3$·diglyme (Hhfa = 1,1,1,5,5,5-hexafluoroacetyacetone, diglyme = $CH_3O(CH_2CH_2O)_2CH_3$) solutions. Microstructure, thermal behaviour and photoluminescent properties of undoped and Eu-doped TiO_2 nanofibrous mats are investigated and compared. To our knowledge, only a few papers report on electrospun Eu-doped PVP-TiO_2 nanohybrids prepared adopting a metal-organic precursor [24]. The use of metalorganic precursors shows some advantages related to their purity (hence a better reproducibility) and to a better solubility in PVP and in non aqueous solvents.

2. Experimental

Polyvinylpyrrolidone (PVP, Aldrich, MW 1300000) solution (7 wt%) was prepared dissolving PVP powder in ethanol at room temperature under magnetic stirring. Then, TiO_2 precursor solution was prepared, by mixing 1.5 g of titanium tetraisopropoxide ($Ti(O\text{-}i\text{-}Pr)_4$, Aldrich) with 3 ml of acetic acid and 3 ml of ethanol and stirring for 10 minutes. The resulting mixture was added to 7.5 ml of PVP solution, previously prepared and stirred for further 10 min. Europium doped TiO_2 source solution was made by mixing to the $Ti(O\text{-}i\text{-}Pr)_4$ solution, the 5 mol.% of $Eu(hfa)_3$·diglyme.

Viscosity of all polymeric solutions was measured at 25°C by a digital viscosimeter (Brookfield DV-II+, Middleboro, MA, USA), using a SC4-21 spindle at 20 rpm. Conductivities were evaluated at 25 °C (CDM230, Analitica De Mori, Italy).

The solution was poured into a glass syringe (Hamilton, Carlo Erba), equipped with a 21 G needle, fixed in a digitally controlled syringe pump (KD Scientific, MA, USA). The needle was connected to a high-voltage supply (Spellman, Model SL 30, NY, USA) that is capable of generating DC voltages up to 30 kV. The solution was electrospun in air in the following conditions: tension 15 kV, needle-target distance 5 cm, feed rate 1 ml/h. Electrospun mats were dried under vacuum for 24 h. The resulting mats were designed as PVP, PVP/TiO_2, PVP/TiO_2:Eu. Undoped and Eu-doped PVP/TiO_2 precursor mats were finally calcinated in air at 500°C for 3 h (heating rate 5°C/min, cooling rate 2°C/min), aimed to remove the polymeric component (TiO_2 and TiO_2:Eu).

Morphology was investigated by scanning electron microscopy technique (SEM, Cambridge Stereoscan 300, United Kingdom) and the average fiber diameter was estimated using a CAD software (on ~100 fibers selection). X-ray diffraction (XRD) (Philips X'Pert 1710) (Cu-Kα radiation, λ = 1.5405600 Å, 10-80° 2Θ, step size 0.020°, time per step 2s, scan speed 0.005°/s) measurements were made on both as-spun and calcinated materials. Phase evolution of as-spun membranes was investigated by variable temperature Θ-2Θ XRD measurements (HT-XRD) (Anton Paar HTK 1200) using the Cu-Kα radiation λ = 1.5405600 Å, and a heating rate of 5°C/min., up to a temperature of 1100°C.

The thermal behaviour was investigated by a simultaneous TG-DTA analysis (Netzsch STA 409) on 60 mg samples with a heating rate of 5°C/min, up to 1250°C.

The spectroscopic characterisation of the as-spun and calcinated samples was performed using laser excited luminescence spectroscopy. The emission spectra were measured using as an excitation source the radiation at 395 nm of a dye laser (Quanta System) pumped with the third harmonic (355 nm) of a Nd-YAG laser (Quanta System pulsed). The emission radiation was collected by using an optical fibre and dispersed with a 0.46 m monochromator (Jobin-Yvon HR460) equipped with a 150 lines/mm (for low resolution luminescence spectra) or with a 1200 lines/mm (for high resolution luminescence spectra) grating. An air cooled CCD device (Jobin-Yvon Spectrum One) was employed to detect the emission radiation. The resolution of the luminescence spectra is ±1 nm. All the spectroscopic measurements were performed at room temperature.

3. Results and discussion

Viscosity and conductivity results are presented in Table 1. Compared to the neat PVP solution, the viscosity of PVP/TiO_2 and PVP/TiO_2-Eu precursor solutions remarkably decrease down to about 23-44 cP vs. 68 cP, due to the addition of TiO_2 precursor sol.

The conductivity of the PVP solution was 4 $\mu S \cdot cm^{-1}$; in the case of PVP/TiO_2-based precursor solutions the conductivity remarkably increased up to 59-64 $\mu S \cdot cm^{-1}$. It has been experimentally demonstrated that this effect has to be attributed to the admixture of the $Ti(O\text{-}i\text{-}Pr)_4$.

Table 1. Viscosity and conductivity of PVP solution, undoped PVP/TiO_2 and Eu-doped PVP/TiO_2 precursor solutions.

Precursor Solution	Viscosity [cP]	Conductivity [$\mu S \cdot cm^{-1}$]
PVP	68	4 ± 1
PVP/TiO_2	23	59 ± 1
PVP/TiO_2:Eu	44	64 ± 0.7

SEM micrographs (Figs. 1-3) showed that PVP, undoped and Eu-doped PVP/TiO_2 precursor mats consisted of defect-free, randomly oriented fibers of fairly uniform diameter. Large interconnected voids were present among the fibers, resulting in a 3D porous network.

The average diameter of as-spun nanofibers was 500 ± 100 nm, 60 ± 15 nm, and 125 ± 50 nm for neat PVP, PVP/TiO_2, and PVP/TiO_2:Eu precursor mats, respectively (Figs. 1 and 2). The remarkable reduction of fiber size observed for all PVP/TiO_2 precursor solution has to be associated with the higher conductivity of the respective spun solutions (Table 1).

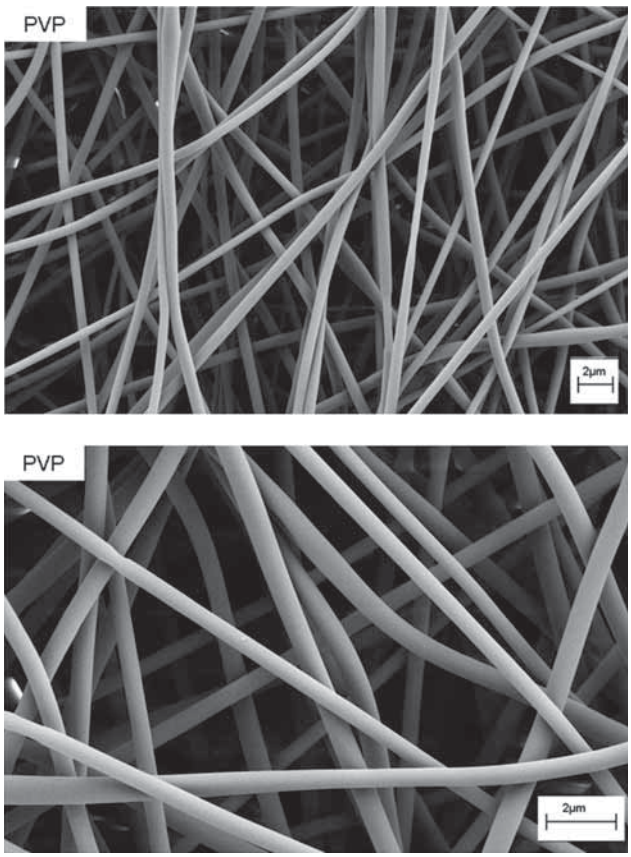

Fig. 1. SEM micrographs of neat PVP.

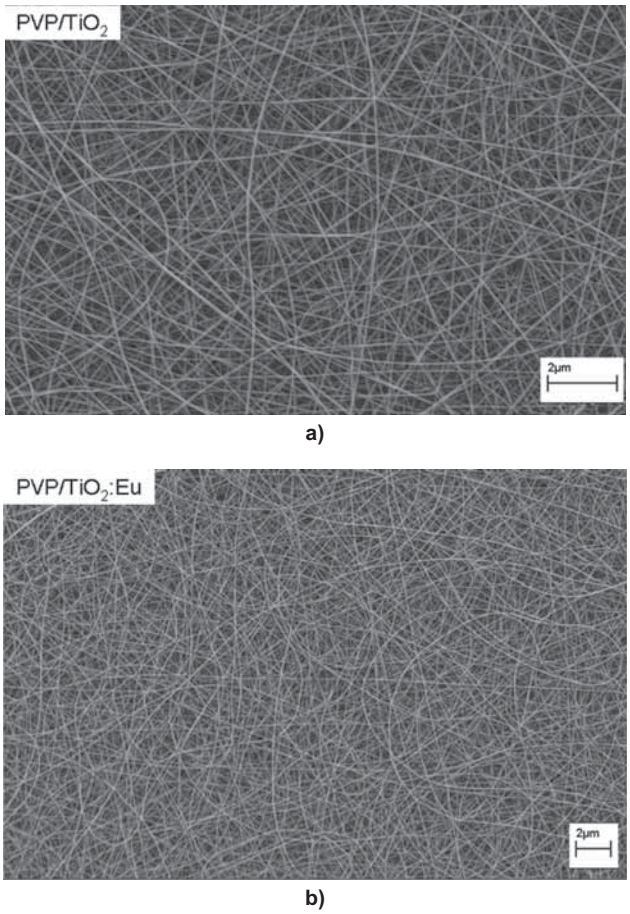

Fig. 2. SEM micrographs of as spun PVP/TiO_2 precursor mats: a) undoped and b) Eu-doped.

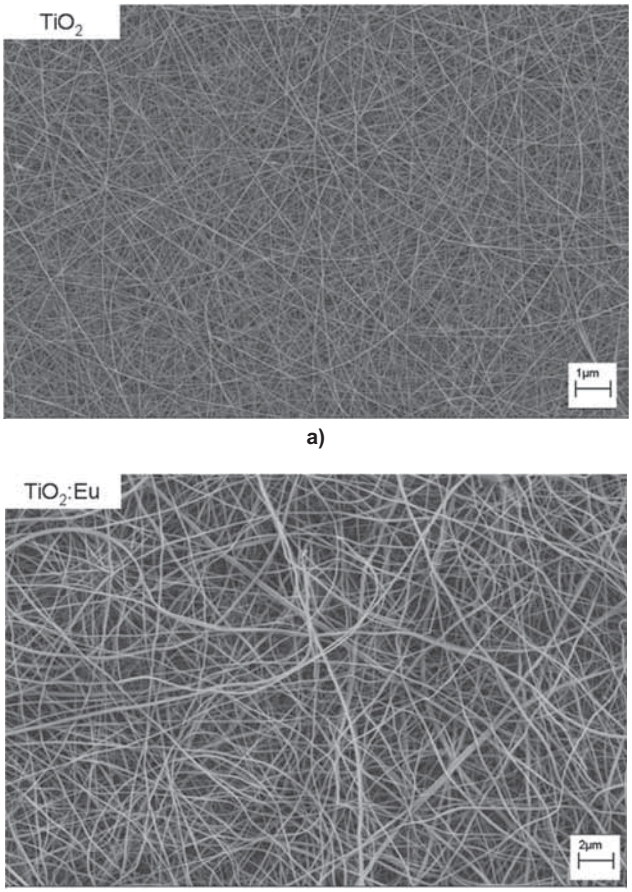

Fig. 3. SEM micrographs of TiO_2 electrospun mats calcinated at 500°C: a) undoped and b) Eu-doped.

Upon thermal treatment at 500°C, nano-sized fibers were obtained having an average diameter of 40 ± 10 nm for the neat TiO_2 (Fig. 3a) and of 80 ± 20 nm for the Eu-doped sample (Fig. 3b).

In Figs. 4a and 4b, TG-DTA curves of the PVP, PVP/TiO_2 and PVP/TiO_2:Eu mats are reported. All the samples showed a weight loss around 100°C, related to the loss of physically absorbed moisture and/or of remaining solvent still present within the fibers. The neat PVP underwent a mass loss in the range 300-600°C corresponding to the PVP combustion and decomposition [4, 26-27]. The decomposition of hybrid electrospun PVP/TiO_2 mats occurred at lower temperature (*i.e.*, 250-500°C), further shifted to even lower temperatures in the Eu-doped samples.

The DTA curves show the expected exothermic peaks associated with these processes. In particular, the exothermic peaks might be associated with Ti-OH decomposition and Ti-O-Ti amorphous network formation (280°C) and with the PVP decomposition (300-400°C) (Fig. 4b) [4, 28-29]. It is worth noting that the progressive lowering of the thermal decomposition temperatures of the PVP matrices (from 600°C for neat PVP to 500°C for the Eu^{3+} doped PVP/TiO_2 sample) observed upon admixing TiO_2 with Eu_2O_3 might be correlated to catalytic properties of both metal centers. Moreover, the pure Eu(hfa)$_3$diglyme sublimates in a single step in the temperature range 113-255°C [30], and therefore it is possible to assume europium dopant as fully incorporated in TiO_2 amorphous phase.

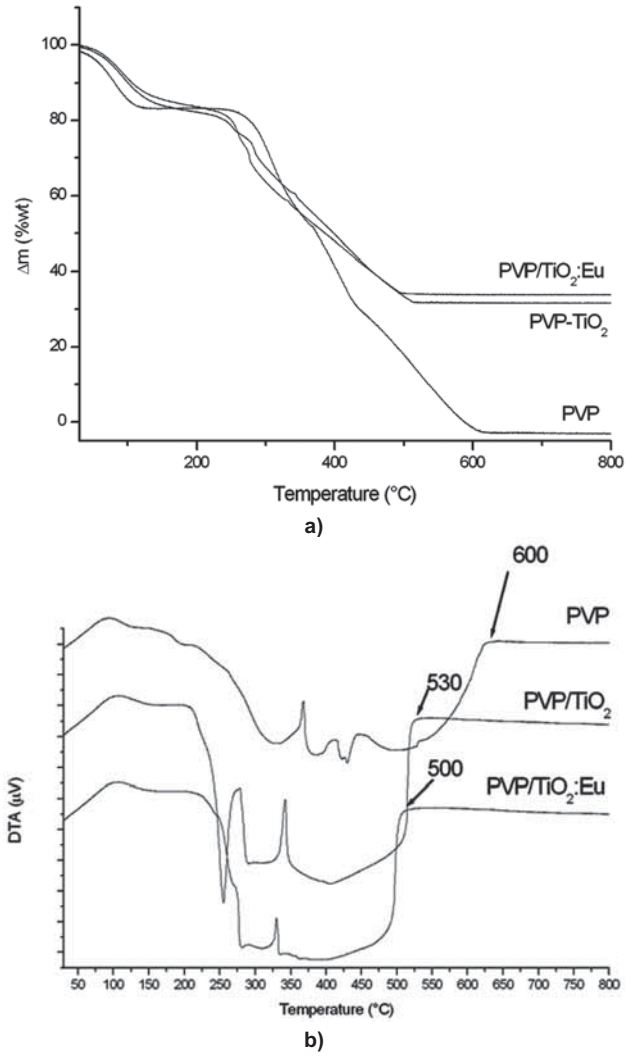

Fig. 4. TG-DTA analysis of PVP, PVP/TiO_2 and PVP/TiO_2:Eu doped electrospun mats: a) TG curves and b) DTA curves.

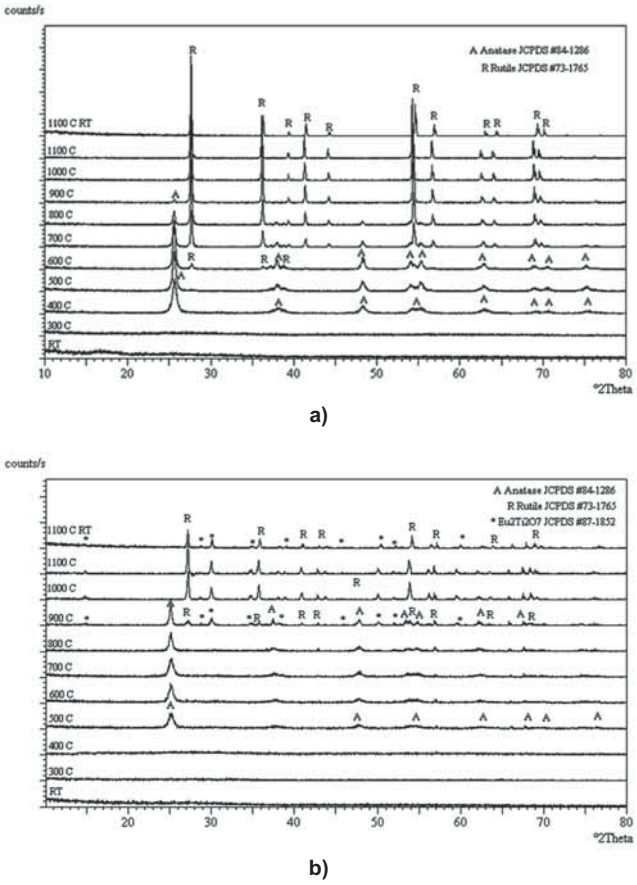

Fig. 5. HT-XRD patterns of samples pre-treated at 300°C: a) PVP/TiO_2 and b) PVP/TiO_2:Eu.

In order to follow the mats phase evolution, high-temperature XRD (HT-XRD) measurements were performed. For pure TiO_2 sample, the crystallization of anatase phase (JCPDS #84-1286) occurred at about 400°C. The phase transition anatase-rutile (JCPDS #73-1765) started at about 600°C, and was completed at around 1000°C, as shown in Fig. 5a.

In the case of Eu-doped mat, a remarkable shift of anatase phase crystallization and phase transition anatase-rutile to higher temperatures is observed (Fig. 5b). The phase transition anatase-rutile phase is evidently delayed, occurring at about 900°C. In fact, the Europium incorporation within titania lattice has a strong inhibition effect for the phase transformation compared with pure titania [22]. It is worth underlining that in the case of the Eu-doped TiO_2 mat any substitutional Eu^{3+} ion certainly causes lattice site distortion, due to the large difference of ionic radii between Ti^{4+} (0.745 Å) and Eu^{3+} (1.087 Å) [28]. For undoped TiO_2, anatase and rutile phases co-existed in a wide temperature range, *i.e.*, from 600 to 900°C. On the other hand, in the case of Eu-doped titania nanofibers, the two polymorphs co-existed only around the transition temperature at about 900°C. Thus the inhibition of the phase transition can be ascribed to the formation of Ti-O-Eu interaction that segregates the Ti-O species at the interface with the TiO_2 domains [9]. Many authors highlighted the effects of rare earth doping on the anatase-rutile (A-R) TiO_2 phase transition rates due to perturbation in the crystal nucleation process for the either substitutional or interstitial dopant ion incorporation within host lattice [4, 28-29].

Moreover, XRD spectra of Eu-doped TiO_2 mat showed at 900°C some extra reflections, associated with the formation of the face centred cubic $Eu_2Ti_2O_7$ (JCPDS #87-1852) as an additional phase. As suggested by other authors [4, 9, 29], this effect is ascribed to enhancement of defects for high lanthanide content samples. The formation of the europium titanate may catalyze mass transport to the nucleation region of the rutile phase, promoting rutile nuclei growth, and therefore promoting the A-R phase transformation [4, 9].

The room temperature emission spectra for the as-spun and annealed at 500°C Eu^{3+} doped nanofibers were measured in the 550-750 nm range upon laser excitation at 395 nm and they are shown in Figs. 6a and 6b. Characteristic emissions due to Eu^{3+} 4*f*-4*f* transitions from the $^5D_0$ excited level to ^7F_J manifolds of the $4f^6$ configuration are present in the spectra. Besides a strong emission attributed to the $^5D_0 \rightarrow {}^7F_2$ transition of Eu^{3+}, additional bands attributed to the transitions $^5D_0 \rightarrow {}^7F_0$ (around 580 nm), $^5D_0 \rightarrow {}^7F_1$ (around 595 nm), $^5D_0 \rightarrow {}^7F_2$ (around 615 nm), $^5D_0 \rightarrow {}^7F_3$ (around 652 nm) and $^5D_0 \rightarrow {}^7F_4$ (around 700 nm) are observed for all the samples.

The red colour of the strong luminescence signal is seen by the naked eye, due to the $^5D_0 \rightarrow {}^7F_2$ transition. The emission bands are broad and transitions between the $^5D_0$ and the ^7F_J Stark levels are not clearly resolved. This behaviour points to a relevant disorder environment around the Eu^{3+} ions.

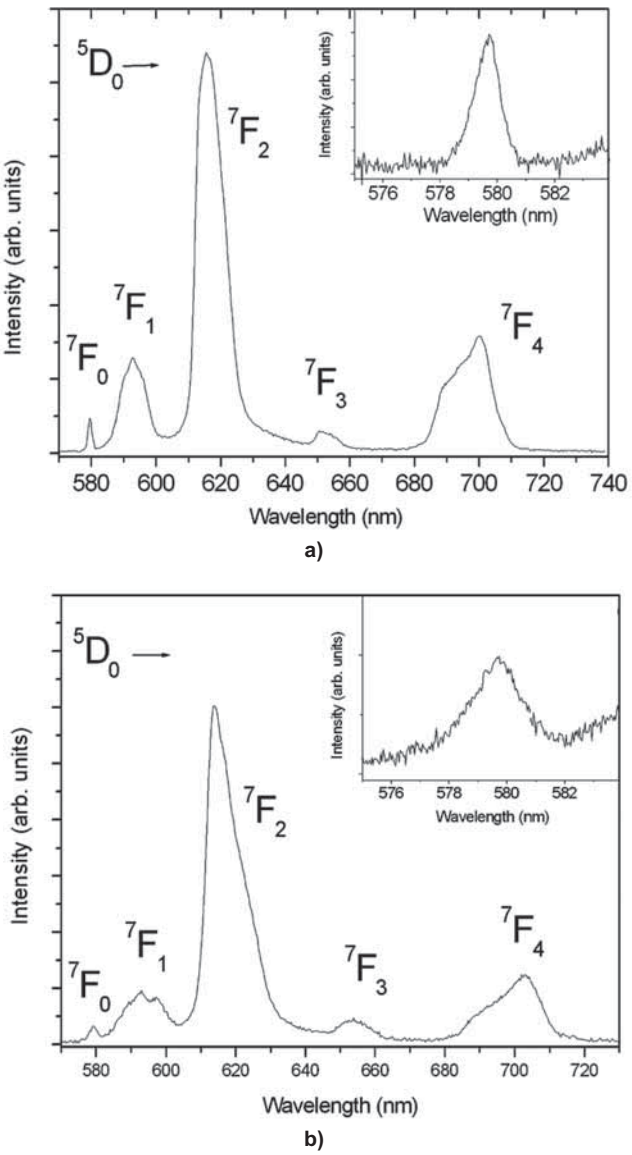

Fig. 6. Room temperature emission spectra for the Eu^{3+} doped PVP/TiO_2 nanofibers: a) as-spun and b) heat treated at 500°C.

4. Conclusions

Eu-doped TiO_2 nanofibers were successfully pursued by electrospinning, using an Eu^{3+} concentration of 5 mol.% The average fiber size was about 40 nm and 80 nm for neat and Eu doped TiO_2 fibers, respectively. The XRD analysis confirms that the rare earth doping delays the crystallisation of the anatase phase and the anatase to rutile phase transition. The formation of europium-titanium oxide ($Eu_2Ti_2O_7$) occurred at 900°C. Upon laser excitation, the europium doped fibers show a strong red luminescence emission due to $4f \rightarrow 4f$ transitions of the Eu^{3+} ions. The relevant broadening of the emission bands points to a notable disorder environment around the lanthanide ions in the host.

Acknowledgements

The Authors wish to thank Fondazione Cariverona (Verona, Italy) for funds supporting.

References

[1] B. Chi, Victorio E. S., Jin T.: Nanotechnology, 17, (2006), 2234-2241.
[2] Prociow E.L., Domaradzki J., Podhorodecki A., Borkowska A., Kaczmarek D., Misiewicz J.: Thin Solid Films, 515, (2007), 6344-6346.
[3] Jeon S., Braun P.V.: Chem. Mater., 15, (2003), 1256-1263.
[4] Zhang Y., Zhang H., Xu Y., Wang Y.: J. Solid State Chem., 177, (2004), 3490.
[5] Teye-Mensah R., Tomer V., Kataphinan W., Tokash J.C., Stojilovic N., Chase G.G., Evans E.A., Ramsier R.D., Smith D.J., Reneker D.H. : J. Phys. Condens. Matter., 16, (2004), 7557.
[6] Jia C.W., Zhao J.G., Duan H.G., Xie E.Q.: Mater. Lett., 61, (2007), 4389.
[7] Ismail A.A., Abboudi M., Holloway P., El-Shall H.: Mater. Res. Bull., 42, (2007), 137.
[8] Zhang H., Song H., Dong B., Han L., Pan G., Bai X., Fan L., Lu S., Zhao H., Wang F., J.: Phys. Chem. C, 112, (2008), 9155.
[9] Zhang Y., Zhang H., Xu Y., Wang Y.: J. Mater. Chem., 13, (2003), 2261.
[10] Zeng Q.G., Zhang Z.M., Ding Z.J., Wang Y., Sheng Y.Q.: Scripta Mater., 57, (2007), 897.
[11] Conde-Gallardo A., Garcıa-Rocha M., Hernandez- Calderon I.: Appl. Phys. Lett., 78, (2001), 3436.
[12] Gutzov S., Bredol M., Wasgestian F.: J. Phys. Chem. Solids, 59, (1998), 69.
[13] Birkhahn R., Garter M., Steckl A.J.: Appl. Phys. Lett., 74, (1999), 2161.
[14] Heikenfeld J., Garter M., Lee D.S., Birkhahn R., Steckl A.J.: Appl. Phys. Lett., 75, (1999), 1189.
[15] Liu Z., Zhang J., Han B., Du J., Mu T., Wang Y., Sun Z.: Micropor. Mesopor. Mater., 81, (2005) 169.
[16] Li D., Xia Y.: Nano Lett., 3, (2003), 555.
[17] Bender E.T., Katta P., Chase G.G., Ramsier R.D.: Surf. Interface Anal., 38, (2006), 1252.
[18] Onozuka K., Ding B., Tsuge Y., Naka T., Yamazaki M., Sugi S., Ohno S., Yoshikawa M., Shiratori S.: Nanotechnology, 17, (2006), 1026.
[19] Nakane K., Yasuda K., Ogihara T., Ogata N., Yamaguchi S.: J. App. Polymer Sci., 104, (2007), 1232.
[20] Tomer V., Teye-Mensah R., Tokash J.C., Stojilovic N., Kataphinan W., Evans E.A., Chase G.G., Ramsier R.D., Smith D.J., Reneker D.H.: Solar Energy Mater. Solar Cells, 85, (2005), 477.
[21] Bender E.T., Wang R., Aljarrah M.T., Evans E.A., Ramsier R.D.: J. Vacuum Scie. Tech. A, 25, (2007) 922.
[22] Zhao J., Jia C., Duan H., Sun Z., Wang X., Xie E.: J. Alloys Comp., 455, (2008), 497.
[23] Zhao J., Duan H., Ma Z., Liu L., Xie E.: J. Optoelectr. Adv. Mater., 10, (2008), 3029.
[24] Wang H., Wang Y., Yang Y., Li X., Wang C.: Mater. Res. Bull., 44, (2009), 408.
[25] Teo W.E., Ramakrishna S.: Nanotechnology, 17, (2006), R89.
[26] Sigmund W., Yuh J., Park H., Maneeratana V., Pyrgiotakis G., Daga A., Taylor J., Nino J.C.: J. Am. Ceram. Soc., 89, (2006), 395.
[27] Watthanaarun J., Supaphol P., Pavarajarn V.: J. Nanosci. Nanotech., 7, (2007), 2443.
[28] Yang H., Zhang K., Shi R.: J. Am. Ceram. Soc., 90, (2007), 1370.
[29] Setiawati E., Kawano K.: J. Alloys Comp., 451, (2008), 293.
[30] Malandrino G., Bettinelli M., Speghini A., Fragala' I.L.: Eur. J. Inorg. Chem., (2001), 1039.

♦

Received 29 April 2010; accepted 26 May 2010